A Mathematical Model for the Dissolution of Particles in Multi-Component Alloys

F.J. Vermolen, C. Vuik

Modelling, Analysis and Simulation (MAS)

MAS-R9822 October 1998

Report MAS-R9822
ISSN 1386-3703

CWI
P.O. Box 94079
1090 GB Amsterdam
The Netherlands

A Mathematical Model for the Dissolution of Particles in Multi-Component Alloys

Fred Vermolen

CWI

P.O.Box 94079, 1090 GB Amsterdam, The Netherlands

Kees Vuik

Faculty of Technical Mathematics and Informatics

Delft University of Technology

P.O.Box 5031, 2600 GA Delft, The Netherlands

ABSTRACT

Dissolution of stoichiometric multi-component particles is an important process ocurring during the heat treatment of as-cast aluminium alloys prior to hot extrusion. A mathematical model is proposed to describe such a process. In this model equations are given to determine the position of the particle interface in time, using a number of diffusion equations which are coupled by nonlinear boundary conditions at the interface. This problem is known as a vector valued Stefan problem. Moreover the well-posedness of the moving boundary problem is investigated using the maximum principle for the parabolic partial differential equation. Furthermore, for an unbounded domain and planar co-ordinates an analytical asymptotic approximation based on self-similarity is derived. Moreover, this self-similar solution and the asymptotic approximation are extended to the vector valued Stefan problem. The approaches are compared to each other and the asymptotic approximation is used to gain insight into the influence of all components on the dissolution. Subsequently a numerical treatment of the vector valued Stefan problem is described. The numerical method is compared with solutions by analytical methods. Finally, an example is shown.

1991 Mathematics Subject Classification: 35A35, 35R35, 65M06, 80A22
Keywords and Phrases: self-similar solution, vector valued Stefan problem, alloy homogenisation, finite differences, (discrete) Newton Raphson method, Jacobian
Note: The paper has been submitted to the European Journal of Applied Mathematics.

1. Introduction

Heat treatment of metals is often necessary to optimise their mechanical properties both for further processing and for final use. During the heat treatment the metallurgical state of the alloy changes. This change can either involve the phases being present or the morphology of the various phases. Whereas the equilibrium phases can be predicted quite accurately from the thermodynamic models, until recently there were no general models for microstructural changes nor general models for the kinetics of these changes. In the latter cases both the initial morphology and the transformation mechanisms have to be specified explicitly. One of these processes that is amenable to modelling is the dissolution of secondary (multi-component) phase particles in a matrix with a given initial composition.

To describe this particle dissolution in solid media several physical models for binary alloys have been developed, incorporating the effects of long-distance diffusion [40, 2, 28] and non-

equilibrium conditions at the interface [23, 1, 30]. These articles did not cover the technologically important dissolution of stoichiometric multi-component particles in multi-component alloys.

The phase transformation element in steel has been studied in [13, 36]. Reiso et al [26] investigated the dissolution of Mg_2Si-particles in aluminium alloys mainly experimentally. They compared their results to a simple dissolution model valid for dissolution in infinite media. Hubert [15] studied the dissolution and growth of second phase particles, consisting of AlN in an iron-based ternary alloy. His analysis was carried out to predict the size of second phase particles during hot-rolling of steel. His model was based on similar physical assumptions as in this paper. However, his approach was purely numerical. The numerical method of [15] differs significantly from the method presented in this paper and is applicable to compounds of maximally two alloying elements. Vermolen et al [31] proposed a numerical method, based on a Newton-Raphson iteration for the computation of the dissolution in ternary alloys. They also analysed the properties of this Stefan problem in terms of existence, uniqueness and monotonicity of the solution and well-posedness of the model [32], [31]. Some physical implications of the model are described in [33] and applications in aluminium and steel industry are given in respectively [34] and [15].

All analyses indicate that the addition of more alloying elements can influence the dissolution kinetics strongly. The present paper describes the dissolution of spherical and needle shaped particles, a planar medium, a spherical layer of segregation and the combination of a dissolving particle and a dissolving spherical layer of segregation in multi-component alloys. In many metallurgical situations, the thermal treatment also aims at the dissolution of the segregation layer around the grains.

The present work covers a Stefan problem in which the growth or dissolution of the particle is determined by diffusion of several chemical elements in the primary phase. This Stefan problem is referred to as a vector valued Stefan problem. The analysis of the vector valued Stefan problem is done in terms of:

- A mathematical model for particle dissolution which leads to a vector valued Stefan problem,
- Fundamental properties of the (scalar) Stefan problem,
- The extension of a self-similarity solution of the scalar Stefan problem to a vector valued Stefan problem,
- An asymptotic limit for the vector valued Stefan problem,
- A numerical method to solve vector valued Stefan problems,
- An application to a three component $Al-Mg-Si$-system.

2. A model of dissolution in multi-component alloys

Consider $n+1$ chemical species denoted by $Sp_i,\ i \in \{1,...,n+1\}$. The dissolution of a $\Pi_{i=1}^{n+1}(Sp_i)_{m_i}$ particle in an $Sp_1,...,Sp_{n+1}$ alloy is investigated. In this formula m_i denote the stoichiometry (composition) of the particle. We divide the material into cells in which a particle dissolves in an Sp_{n+1}-rich phase. It is assumed that the overall concentrations of

$Sp_i,\ i \in \{1,...,n\}$ are small with respect to the concentration of component Sp_{n+1}. The concentrations are written as c_i (mol/m^3), $i \in \{1,...,n\}$. At a given temperature the initial concentrations in the Sp_{n+1}-rich phase are equal to $c_i^0,\ i \in \{1,...,n\}$. The composition of the components in the particle are denoted by $c_i^{part},\ i \in \{1,...,n\}$. We assume the particle concentrations to be fixed. The interface concentrations c_i^{sol} are variant. As an example consider the dissolution of an Mg_2Si particle in an Al-rich phase. Then $Sp_1 = $ Mg, $Sp_2 = $ Si, and $Sp_3 = $ Al. The values of m_1 and m_2 are 2, 1 respectively, and $n = 2$.

We consider a one-dimensional problem. The geometry is given by $\Omega(t) = \{r \in \mathbb{R} | M_L \leq S_L(t) < r < S_R(t) \leq M_R\},\ t \in [0,T]$ where T is an arbitrary positive number. In some applications there is a time t_L and t_R such that respectively $S_L(t) = M_L, t \geq t_L$ and $S_R(t) = M_R, t \geq t_R$. For the determination of c_i we use the multi-component version of Fick's Second Law (see [33], [24] p. 160). For simplicity we assume that all species diffuse independently, and that the diffusion coefficients $\mathbb{D}_i,\ i \in \{1,...,n\}$ (m^2/s) are constant. The resulting equations are:

$$\frac{\partial c_i}{\partial t} = \frac{\mathbb{D}_i}{r^a}\frac{\partial}{\partial r}(r^a \frac{\partial c_i}{\partial r}),\quad r \in \Omega(t),\quad t \in (0,T],\quad i \in \{1,...,n\}, \tag{2.1}$$

where a is a geometric parameter, which equals 0,1, or 2 for respectively a planar, a cylindrical, or a spherical geometry. Note that M_L should be non-negative for $a \neq 0$. All these geometries occur in metallurgical applications. As initial conditions we use

$$c_i(r,0) = c_i^0(r),\quad r \in \Omega(0),\quad i \in \{1,...,n\}, \tag{2.2}$$

where c_i^0 are given non-negative functions. When a moving boundary becomes fixed, we assume that there is no flux through the boundary, so

$$\frac{\partial c_i}{\partial r}(M_k,t) = 0,\quad \text{for } t \geq t_k,\quad i \in \{1,...,n\},\quad k \in \{L,R\}. \tag{2.3}$$

It is possible that the particles contain different chemical species. In the following we assume that particle k contains n_k chemical species with indices in $\Phi_k \subset \{1,...,n+1\},\ k \in \{L,R\}$. The complement of Φ_k is defined as $\Phi_k^c = \{1,...,n+1\} \setminus \Phi_k$. On the moving boundaries the following conditions and definitions are used:

$$\frac{\partial c_i}{\partial r}(S_k(t),t) = 0,\quad t \in [0,T],\quad i \in \Phi_k^c,\quad k \in \{L,R\}, \tag{2.4}$$

and

$$c_{i,k}^{sol}(t) := c_i(S_k(t),t),\quad t \in [0,t_k],\quad i \in \Phi_k,\quad k \in \{L,R\}. \tag{2.5}$$

So $2 + n_L + n_R$ unknown quantities remain: $S_k(t)$, and $c_{i,k}^{sol}(t),\quad i \in \Phi_k,\quad k \in \{L,R\}$. To obtain a unique solution $2 + n_L + n_R$ boundary conditions are necessary. We assume that the particles are stoichiometric, which means that the concentrations $c_{i,k}^{part}$ in the particles are constant. Using the Gibbs free energy of the stoichiometric compound we get [33]:

$$\Pi_{i \in \Phi_k}(c_{i,k}^{sol}(t))^{m_i} = K_k,\quad t \in (0,t_k),\quad k \in \{L,R\}, \tag{2.6}$$

where K_k are constants. The balance of atoms and the constant composition of the particle lead to the following equations for the moving boundary positions:

$$(c_{i,k}^{part} - c_{i,k}^{sol}(t))\frac{dS_k}{dt}(t) = \mathbb{D}_i \frac{\partial c_i}{\partial r}(S_k(t),t),\quad t \in (0,t_k],\quad i \in \Phi_k,\quad k \in \{L,R\}. \tag{2.7}$$

Condition (2.7) implies

$$\frac{\mathbb{D}_i}{c_{i,k}^{part} - c_{i,k}^{sol}(t)} \frac{\partial c_i}{\partial r}(S_k(t),t) = \frac{\mathbb{D}_j}{c_{j,k}^{part} - c_{j,k}^{sol}(t)} \frac{\partial c_j}{\partial r}(S_k(t),t), \quad i,j \in \Phi_k, \quad k \in \{L,R\}. \tag{2.8}$$

The moving boundary problem given by equations (2.1),..., (2.7) is known as a Stefan problem. We define the space Q as $Q := \{(r,t) \in \Omega(t), t \in (0,T)\}$. We look for solutions of the Stefan problem with the following properties: $S \in C^1(0,T]$ and $c_i \in C^{2,1}(Q) \cap C(\bar{Q})$. When $c_i^0(S(0)) \neq c^{sol}(0)$, $i \in \{1..n\}$, then c_i cannot be required to be continuous in $(S(0),0)$. In these points, we require:

$$\min\{c_i^0(S(0)), c_i^{sol}(0)\} = \liminf_{\substack{(r,t)\in Q \\ (r,t)\to(S(0),0)}} c_i(r,t) \leq \limsup_{\substack{(r,t)\in Q \\ (r,t)\to(S(0),0)}} c_i(r,t) = \max\{c_i^0(S(0)), c_i^{sol}(0)\},$$

compare Friedman [12]. For a recent book where this type of problems is considered we refer to [35] (see for instance p. 132 (2.5), (2.9)). There are some differences between the dissolution in a binary alloy and in a multi-component alloy. In the first place, n diffusion equations have to be solved, which are coupled through the conditions (2.5), (2.6), and (2.7) on the moving boundaries. Secondly, the problems are nonlinear due to the balance of atoms on S_L, S_R, both in the binary and the multi-component case. However, in the mathematical model for a multi-component alloy an extra non-linearity occurs in equation (2.6). Survey papers and books on the Stefan problem are: [10], [14], [18], [8], [19], and [5].

3. Properties of the scalar d-dimensional Stefan problem

In this section first the maximum principle is formulated. Using this maximum principle the well-posedness of the Stefan problem is discussed. It is proven that there are Stefan problems for which no solution exists. The properties and solution of the Stefan problem are first discussed for the case of one diffusing element, therefore the subscript for the index of the alloying element is omitted. For completeness, we pose the general multi-dimensional scalar Stefan problem.

We consider diffusion in the primary phase domain, $\Omega(t) \subset \mathbb{R}^d$, in which diffusion of a chemical element takes place. This domain encloses and / or is enclosed by the particle, of which the domain is denoted by $P(t)$. The initial concentration in the primary phase domain is given by $c(\underline{r},0) = c^0$, $\forall \underline{r} \in \Omega(0)$. For the concentration, we have in $\Omega(t)$:

$$\frac{\partial c}{\partial t} = \mathbb{D}\nabla\left(\nabla c\right), \quad \underline{r} \in \Omega(t),\, t \in (0,T]. \tag{3.1}$$

For the concentration inside the particle, $P(t)$, we have:

$$c(\underline{r},t) = c^{part}, \quad \underline{r} \in P(t),\, t \in (0,T]. \tag{3.2}$$

As boundary conditions, we have at the moving boundary ($S(t) = \overline{\Omega}(t) \cap \overline{P}(t)$):

$$c(\underline{r},t) = c^{sol}, \quad \underline{r} \in S(t),\, t \in (0,T],$$

and the normal component of the velocity of the moving boundary, $v_\nu(t)$, is given by:

$$(c^{part} - c^{sol}) v_\nu(t) = \mathbb{D}\frac{\partial c}{\partial \nu}, \quad \underline{r} \in S(t),\, t \in (0,T], \tag{3.3}$$

and at the fixed boundary, $\Gamma := \partial\Omega \setminus S(t)$, we have a homogeneous Neumann condition, with ν defined as the outward normal:

$$\frac{\partial c}{\partial \nu} = 0, \quad \underline{r} \in \Gamma,\, t \in (0,T].$$

In this section c^{part}, c^{sol} and c^0 are assumed constant. We will now summarise some basic properties of this scalar Stefan problem.

3.1 The maximum principle for the diffusion equation
The Stefan problem is formed by the diffusion equation and a displacement equation for the moving boundary. The solution $c(r,t)$ of the diffusion equation with the above requirements is unique and satisfies a maximum principle:

Maximum principle
Suppose c satisfies the inequality

$$\nabla^2 c - \frac{\partial c}{\partial t} \geq 0, \quad \underline{r} \in \Omega(t), \quad t \in (0,T], \tag{3.4}$$

then a local maximum has to occur at the boundaries, or at $t = 0$ (the initial condition). Suppose that a local maximum occurs at the point P on S or Γ. If $\frac{\partial}{\partial \nu}$ denotes the derivative in an outward direction from $\Omega(t)$, then $\frac{\partial c}{\partial \nu} > 0$ at P.

This statement is referred to as the maximum principle and has been proved by Protter and Weinberger for a general parabolic operator (see [25] p. 168, p. 170) and by Vuik [37] for an unbounded domain (see [37], Lemma 2.4., p. 18). For completeness, we generalise the maximum principle to the presence of a discontinuity at $(S(0),0) \in \bar{Q}$ in the appendix. This principle can also be applied for local minima (and $\frac{\partial c}{\partial \nu} < 0$) when the inequality in (3.4) is reversed. The principle thus requires the global extremes of a solution to the diffusion equation to occur either at the boundaries $S(t), \Gamma$ or at $t = 0$.

From the Stefan-condition (3.3), one can deduce immediately that the normal component of the interface velocity, v_ν has to satisfy:

$$v_\nu(t)(c^{part} - c^{sol})\frac{\partial c}{\partial \nu}(\underline{r},t) > 0, \quad \forall \underline{r} \in S(t),\, t \in (0,T], \quad c^{part} \neq c^{sol} \neq c^0, \tag{3.5}$$

note that $\frac{\partial c}{\partial \nu} \neq 0$ due to the maximum principle and $c^{sol} \neq c^0$.

3.2 Existence of a solution to the Stefan problem
We will analyse the existence of a solution to a class of Stefan problems. Inequality (3.5) will be used in the proof of the existence proposition. First we introduce the following definition:

Definition 3.1 A solution to the Stefan problem is mass-conserving if the solution satisfies:

$$\int_{\Omega(t)\cup P(t)} (c(\underline{r},t) - c^0)dV = \left(c^{part} - c^0\right)\int_{P(0)} dV, \quad \forall t \in (0,T]. \tag{3.6}$$

This definition states that the total mass remains constant in time. Note that $c(\underline{r},t) = c^{part}$, $\underline{r} \in \P(t)$, $t \in (0,T]$. It then can be proven easily that if the solution is mass-conserving

(i.e. (3.6) holds), we have:

$$\frac{\partial c}{\partial \nu} = 0, \forall \underline{r} \in \Gamma, t \in (0,T] \Rightarrow (c^{part} - c^{sol}) v_\nu(t) = \mathbb{D} \frac{\partial c(\underline{r},t)}{\partial \nu} \forall \underline{r} \in S(t),\ t \in (0,T]. \qquad (3.7)$$

Now, we formulate a proposition about the existence of a mass conserving solution.

Proposition 3.1 The problem as constituted as the Stefan problem has no solution if

$$\left(c^{part} - c^0\right)\left(c^{part} - c^{sol}\right) \leq 0,\ \textit{and}\ c^{sol} \neq c^0\ \textit{with}\ c^{part}, c^{sol}, c^0 \in \mathbb{R}^+ \cup \{0\}.$$

Proof

Suppose that a solution exists for the Stefan problem with $\left(c^{part} - c^0\right)\left(c^{part} - c^{sol}\right) < 0$. We then have $c^0 < c^{part} < c^{sol}$ or $c^{sol} < c^{part} < c^0$.

First we consider the case that $c^0 < c^{part} < c^{sol}$. From the maximum principle we then have $\frac{\partial c}{\partial \nu} > 0$. From equation (3.5) and $(c^{sol} - c^0) * \frac{\partial c}{\partial \nu} > 0$, follows that $v_\nu(t) < 0$ and thus the particle grows. Considering $t = 0$, we have for the global mass difference:

$$\int_{\Omega(0) \cup P(0)} (c(\underline{r},0) - c^0) dr = (c^{part} - c^0) \int_{P(0)} dV.$$

For $t > 0$, we have for the global mass difference:

$$\int_{\Omega(t) \cup P(t)} (c(\underline{r},t) - c^0) dV = (c^{part} - c^0) \int_{P(t)} dV + \int_{\Omega(t)} (c(\underline{r},t) - c^0) dV$$

$$= (c^{part} - c^0) \left(\int_{P(0)} dV + \int_{P(t) \setminus P(0)} dV \right) + \int_{\Omega(t)} (c(\underline{r},t) - c^0) dV =$$

$$= (c^{part} - c^0) \int_{P(0)} dV + \int_{\Omega(0)} (c(\underline{r},t) - c^0) dV.$$

From the maximum principle, it follows that $c(\underline{r},t) > c^0$. It is then clear that

$$\int_{\Omega(t) \cup P(t)} (c(\underline{r},t) - c^{sol}) dV = (c^{part} - c^0) \int_{P(0)} dV + \int_{\Omega(0)} (c(\underline{r},t) - c^0) dV > (c^{part} - c^0) \int_{P(0)} dV.$$

This implies that equations (3.7) and (3.6) are not equivalent, according to the definition, the solution is not mass-conserving. The Stefan problem with $c^0 < c^{part} < c^{sol}$ does not have a solution and is therefore ill-posed.

A similar proof can be given to show that for the case $c^{sol} < c^{part} < c^0$ no solution exists either. We then can show that

$$(c^{part} - c^0) \int_{P(t)} dV + \int_{\Omega(t)} (c(\underline{r},t) - c^0) dV < (c^{part} - c^0) \int_{P(0)} dV.$$

Suppose that a solution exists for the Stefan problem with $\left(c^{part}-c^{0}\right)\left(c^{part}-c^{sol}\right)=0$, then we either have $c^{part}=c^{0}$ or $c^{part}=c^{sol}$. For the first case a similar proof as the preceeding one can be used to show that no solution exists. For the second case one can prove that $|v_{\nu}(t)|$ has to blow up in order to keep $|\frac{\partial c(S(t),t)}{\partial \nu}|>0$ as required due to the maximum principle when $c^{sol}\neq c^{0}$ (note the requirements on continuity of c). $\square$

This proposition has been given and proven for a one-dimensional unbounded Stefan problem in [32].

If we have $\left(c^{part}-c^{0}\right)*\left(c^{part}-c^{sol}\right)>0$, we either have $(c^{part}<c^{0})\wedge(c^{part}<c^{sol})$ or $(c^{part}>c^{0})\wedge(c^{part}>c^{sol})$. Then it can be proven in a similar way that it is possible to conserve mass and we then call the Stefan problem well posed. Furthermore, it appears that we will have dissolution, i.e. $v_{\nu}>0$, if $\left(c^{sol}-c^{0}\right)\left(c^{sol}-c^{part}\right)<0$ and contrarily for the other well-posed problems, we will have growth.

4. An asymptotic solution to a planar vector valued Stefan problem

Consider a planar particle that is dissolving in an infinite matrix: $\Omega(t):=\{r\in\mathbb{R}|S(t)<r<\infty\}$. We take $\Phi=\{1,...,n\}$. The diffusion is then given by:

$$\frac{\partial c_i}{\partial t}=\mathbb{D}_i\frac{\partial^2 c_i}{\partial r^2},\quad r\in\Omega(t),\ t\in(0,T],\ i\in\{1,...,n\}.$$

At the interface, we define:

$$c_i(S(t),t)=:c_i^{sol}(t), i\in\{1,...,n\}.$$

At infinity and for $t=0$:

$$c_i(r,0)=c_i^0,\quad c_i(\infty,t)=c_i^0,\quad S(0)=S_0,\ i\in\{1,...,n\}.$$

where c^0 is a given constant.

It can be proven that the solution is [39],[32]:

$$\tilde{c_i}(r,t)=\frac{c_i^0-c_i^{sol}}{\operatorname{erfc}(\frac{k}{2\sqrt{\mathbb{D}_i}})}*\operatorname{erfc}\left(\frac{r-S_0}{2\sqrt{\mathbb{D}_i t}}\right)+c_i^0,\quad r\in\Omega(t),\ t\in(0,T],\ i\in\{1,...,n\}. \tag{4.1}$$

with k as defined in: $S(t)=S_0+k\sqrt{t}$. Note that due to condition (2.8), the value of k does not depend on the chemical element. Combination of (4.1) with (2.7) and the square-root like solutions of the free boundary position $S(t)$, yields the following set of equation to be solved for k and c_i^{sol} for all chemical elements:

$$\frac{k}{2}=\frac{\left(c_i^0-c_i^{sol}\right)}{\left(c_i^{part}-c_i^{sol}\right)}\sqrt{\frac{\mathbb{D}_i}{\pi}}*\frac{\exp\left(-\frac{k^2}{4\mathbb{D}_i}\right)}{\operatorname{erfc}\left(\frac{k}{2\sqrt{\mathbb{D}_i}}\right)},\quad \forall i\in\{1,...,n\}. \tag{4.2}$$

$$\Pi_{i=1}^{n}(c_i^{sol})^{m_i} = K. \tag{4.3}$$

For the scalar Stefan problem this has been analysed in [32]. We solve the system (4.2,4.3) of $n+1$ nonlinear equations for $n+1$ variables $(k, c_i^{sol}, i \in \{1, ..., n\})$ with a numerical method. It turns out that the value of k in the above equation can be approximated by

$$\tilde{k} = 2\frac{\left(c_i^0 - c_i^{sol}\right)}{\left(c_i^{part} - c_i^{sol}\right)} * \sqrt{\frac{\mathbb{D}_i}{\pi}} \tag{4.4}$$

provided that $|\frac{c_i^0 - c_i^{sol}}{c_i^{part} - c_i^{sol}}| << 1,\ \exists i \in \{1, ..., n\}$. The value $\tilde{k}$ leads to the same solution as one would obtain from a (inverse) Laplace transform of the diffusion equation [40], [1]. Before we state the accuracy of (4.4), we define:

$$A_i := \frac{c_i^0 - c_i^{sol}}{c_i^{part} - c_i^{sol}} \cdot \sqrt{\frac{1}{\pi}},$$

$$x_i := \frac{k}{2\sqrt{\mathbb{D}_i}},$$

$$f(x) := \frac{\exp(-x^2)}{\mathrm{erfc}(x)}.$$

It turns out that approximation (4.4) represents a lower limit for the value of k. This is formulated in the following theorem in which the definitions for A_i, x_i and $f(x_i)$ are used:

Theorem 4.1 Let $\frac{x_i}{A_i} = f(x_i)$ for a given, fixed $A_i < \frac{1}{\sqrt{\pi}}$ and $f(x_i)$ as defined above, then:

$$A_i < x_i < \frac{A_i}{1 - \sqrt{\pi} \cdot A_i}.$$

Proof

Using a series expansion of $\frac{f(x)}{x}$ at $x \to \infty$ [32], one obtains (for ease of notation we here omit the index i):

$$lim_{x\to\infty}\frac{f(x)}{x} = \sqrt{\pi}.$$

Furthermore, it is easy to see that:

$$lim_{x\to-\infty} f(x) \downarrow 0.$$

Since $f(x), f'(x), f''(x) > 0, x \in \mathbb{R}$ (f is convex and increases monotonously), one obtains: $0 < f'(x) < \sqrt{\pi}, x \in \mathbb{R}$. With $f(0) = 1$ and from the Mean Value Theorem $\frac{x_i}{A_i} = 1 + x_i \cdot f'(\tilde{x_i}), \tilde{x_i} \in (0, x_i)$, one obtains: $1 < \frac{x_i}{A_i} < 1 + \sqrt{\pi} \cdot x_i$. This implies that:

$$A_i < x_i < \frac{A_i}{1 - A_i \cdot \sqrt{\pi}}. \quad \square$$

We remark that the theorem agrees with the requirement of well-posedness as discussed in Section 3. For the case of a Stefan problem in $\mathbb{R}^1$ (planar geometry) in an infinite domain, one thus can state that the solution is a self-similar solution. Using the above theorem, one can easily show by subtraction of A_i the following on the accuracy of approximation (4.4):

Corollary 4.1 Let $\frac{x_i}{A_i} = f(x_i)$ for a given, fixed A_i and $f(x)$ from the above definition, then:

$$|\frac{x_i - A_i}{x_i}| = O(A_i).$$

When we insert the concentrations into the definitions, one obtains from the theorem:

$$S_0 + 2 \cdot \frac{c_i^0 - c_i^{sol}}{c_i^{part} - c_i^{sol}} \cdot \sqrt{\frac{\mathbb{D}_i t}{\pi}} < S_0 + k \cdot \sqrt{t} < S_0 + 2 \cdot \frac{c_i^0 - c_i^{sol}}{c_i^{part} - c_i^0} \cdot \sqrt{\frac{\mathbb{D}_i t}{\pi}}. \tag{4.5}$$

From inequality (4.5), the velocity of the moving boundary can be approximated by:

$$\frac{\left(c_i^0 - c_i^{sol}\right)}{\left(c_i^{part} - c_i^{sol}\right)} \cdot \sqrt{\frac{\mathbb{D}_i}{\pi t}} < \frac{dS(t)}{dt} < \frac{\left(c_i^0 - c_i^{sol}\right)}{\left(c_i^{part} - c_i^0\right)} \cdot \sqrt{\frac{\mathbb{D}_i}{\pi t}}. \tag{4.6}$$

This (approximate) solution will be used in the remainder of the present paper as a solution of the vector valued Stefan problem since it gives a good insight into the asymptotic behaviour of the solution. It is also noted that this lower bound would be obtained if the interface would be stationary, i.e. not moving [40]. Since the lower bound is only valid for the case that A_i is sufficiently small, one must be careful in its use. Otherwise, the lower bound then may yield solutions that are not mass-conserving (see Section 3 and [31]).

The solutions that have been described here only hold for a planar particle in an infinite domain. Since in real world situations, the domain is finite, we formulate the following proposition concerning the difference between the solution in an infinite and finite domain. For simplicity, we formulate the proposition for one alloying element only and therefore omit the subscript i.

Proposition 4.1 Let c_∞ and c_M be solutions of the diffusion equation on respectively the unbounded and bounded domain ($\Omega_M := \{r \in \mathbb{R} | S(t) < r < M\}$,M<$\infty$) with a homogeneous Neumann boundary condition on the fixed boundary $r = M, t \in (0, T]$, and $c^{sol} > c^0 \geq 0$, then:

$$c_M(r,t) > c_\infty(r,t), \;\; \forall r \in \Omega_M(t),\, t \in (0,T].$$

Proof

Define $w := c_M - c_\infty, r \in \Omega(t), t \in (0,T]$, then

$$\frac{\partial w(r,t)}{\partial t} = \mathbb{D}\frac{\partial^2 w(r,t)}{\partial r^2}, \;\; r \in \Omega(t),\; t \in (0,T],$$

and $w(r,0) = 0, w(S(t),t) = 0$.
Since $c^{sol} > c^0$, one can see $\frac{\partial w(M,t)}{\partial \nu} > 0,\; \forall t \in (0,T]$, with ν denoting the outward normal at $r = M$. According to the maximum principle we only can have extremes at either of the boundaries or at $t = 0$. We now consider two cases:

- Suppose $w(\tilde{r},t) < 0$, for some $\tilde{r} \in (S(t),M]$, we then either have at least one minimum for $r = \tilde{r}$ to satisfy $\frac{\partial w(M,t)}{\partial n} > 0$. This contradicts with the maximum principle.
- Suppose $w(\tilde{r},t) = 0$, for some $\tilde{r} \in (S(t),M]$, since $\frac{\partial w(M,t)}{\partial \nu} > 0$, we have $w(M,t) > 0$ (note that $w(r,t) \in C^{2,1}(Q) \cap C(\bar{Q})$). This contradicts with the maximum principle.

Hence $w(r,t) > 0$, for all $r \in (S(t),M], t \in (0,T]$. So: $\frac{\partial w(M,t)}{\partial \nu} > 0$, and $w(r,t)$ satisfies the maximum principle and hence:

$$c_M - c_\infty > 0, \;\; \forall r \in (S(t),M),\; t \in (0,T],$$

which completes the proof. □

From the above proposition follows that $|\frac{\partial c_\infty(S(t),t)}{\partial r}| > |\frac{\partial c_M(S(t),t)}{\partial r}|$ on $t \in (0,T]$.

Some limitations of vector valued Stefan problems are given in [31]. It appears that the model breaks down when the concentration at the interface equals the concentration in the particle. There it is shown that this happens if $c_i^0 = c_i^{part}$ for some $i \in \Phi$ and $c_j^0 = 0$ for some $j \in \Phi \setminus \{i\}$. Monotonicity properties are described there too.

5. A limit of the solution to a planar vector valued Stefan problem

In this section we consider the consequences of the approximation (4.4, 4.6) as described in Section 4. For this purpose, we take the special situation that

- $c_i^{part} >> c_i^{sol} > c_i^0 = 0,\; \forall i \in \{1,...,n\}$,

Since in metallurgy one often encounters $c_i^{part} >> c_i^{sol} > c_i^0 \approx 0$, the solution that satisfies the above mentioned constraints is referred to as a limit. From the inequalities we see that:

- $-1 << \frac{c_i^0 - c_i^{sol}}{c_i^{part} - c_i^{sol}} < 0$,
- $\frac{c_i^0 - c_i^{sol}}{c_i^{part} - c_i^{sol}} \approx -\frac{c_i^{sol}}{c_i^{part}}$.

From this and equation (4.4), one easily can write down the following recurrent relationship:

$$\frac{-c_i^{sol}}{c_i^{part}} \cdot \sqrt{\mathbb{D}_i} \approx \frac{-c_{i+1}^{sol}}{c_{i+1}^{part}} \cdot \sqrt{\mathbb{D}_{i+1}}, \;\; \forall i \in \{1,...,n-1\}. \tag{5.1}$$

Assuming an equality in equation (5.1) yields an approximate $\tilde{c}_i^{sol}$:

$$\tilde{c}_i^{sol} = \sqrt{\frac{\mathbb{D}_1}{\mathbb{D}_i}} \cdot \frac{c_i^{part}}{c_1^{part}} \cdot \tilde{c}_1^{sol}. \tag{5.2}$$

Substitution of equation (5.2) into the assumption that $\Pi_{i=1}^{n}(c_i^{sol})^{m_i} = K$ and defining $\mu := \Sigma_{i=1}^{n}(m_i)$, one obtains:

$$\left(\frac{\sqrt{\mathbb{D}_1}}{c_1^{part}}\right)^{\mu} \cdot \Pi_{i=1}^{n}\left(\frac{c_i^{part}}{\sqrt{\mathbb{D}_i}}\right)^{m_i} (\tilde{c}_1^{sol})^{\mu} = K. \tag{5.3}$$

The solution to equation (5.3) is:

$$\tilde{c}_1^{sol} = \frac{c_1^{part}}{\sqrt{\mathbb{D}_1}} \cdot K^{\frac{1}{\mu}} \cdot \Pi_{i=1}^{n}\left(\frac{\sqrt{\mathbb{D}_i}}{c_i^{part}}\right)^{\frac{m_i}{\mu}} \tag{5.4}$$

We reject nonpositive solutions and solutions that are not real. Substitution of the unique real, positive solution into equation (4.6), yields:

$$\frac{dS(t)}{dt} \approx -\frac{c_{eff}^{sol}}{c_{eff}^{part}} \cdot \sqrt{\frac{\mathbb{D}_{eff}}{\pi t}}, \tag{5.5}$$

with $c_{eff}^{sol}, c_{eff}^{part}$ and $\mathbb{D}_{eff}$ defined as:

$$c_{eff}^{sol} := K^{\frac{1}{\mu}},$$

$$c_{eff}^{part} := \Pi_{i=1}^{n}(c_i^{part})^{\frac{m_i}{\mu}},$$

$$\mathbb{D}_{eff} := \Pi_{i=1}^{n}(\mathbb{D}_i)^{\frac{m_i}{\mu}}.$$

The symbols c_{eff}^{sol}, c_{eff}^{part}, and $\mathbb{D}_{eff}$ are referred to as respectively the effective solid solubility, effective particle concentration and effective diffusion coefficient. We thus have approximated the solution to a vector valued Stefan problem with a solution to a scalar Stefan problem. In other words the dissolution of a multi-component particle can be described by the dissolution of a particle in a quasi-binary alloy. One can integrate equation (5.5) in time to yield:

$$S(t) \approx S_0 - 2 \cdot \frac{c_{eff}^{sol}}{c_{eff}^{part}} \cdot \sqrt{\frac{\mathbb{D}_{eff}t}{\pi}}. \tag{5.6}$$

This case holds for the assumptions that the particle concentrations are much larger than the concentration at the moving boundary. Moreover, the initial concentration in the primary phase has to be equal to zero. Nevertheless, equation (5.5) gives a good insight into the influence of the addition of an alloying element to the dissolution kinetics. The approximation may be used to test the results from the more general numerical solution. For the case in which the particle concentrations of all alloying elements are equal, i.e. $c_i^{part} = c^{part}$ and $m_i = 1,\ \forall i \in \{1, ..., n\}$, one can simplify the effective quantities to yield for this very special case:

$$c_{eff}^{sol} := (K)^{\frac{1}{n}},\ \ c_{eff}^{part} := c^{part},\ \ \mathbb{D}_{eff} := (\Pi_{i=1}^{n}\mathbb{D}_i)^{\frac{1}{n}}.$$

It can now be seen that the effective diffusion coefficient is equal to the geometric mean of all the diffusion coefficients of the alloying elements.

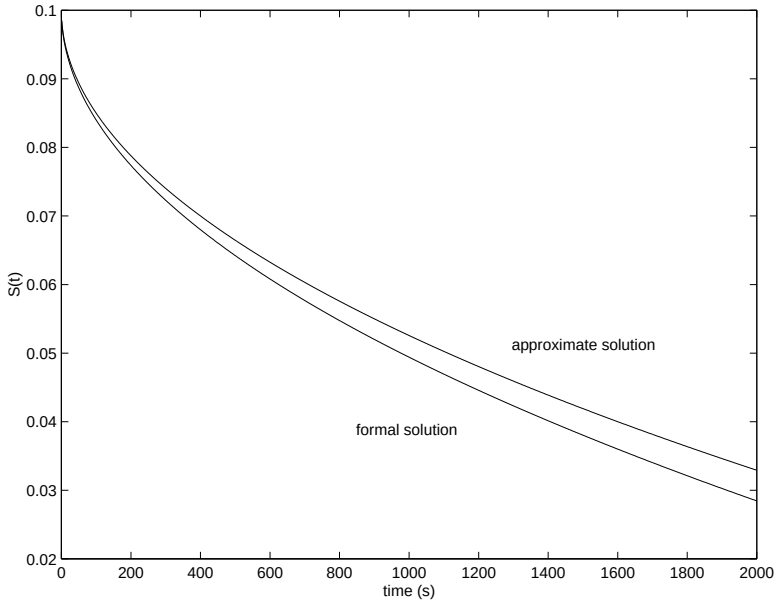

Figure 1: Two analytical approaches compared.

To clarify this quasi-binary approach we compare this approach to the more general approach as described in Section 4. We take the following hypothetic quantities: $c_i^0 = 0$, $c_i^{part} = 33 mol/m^3, \mathbb{D}_i = i \cdot 10^{-3}$ and $m_i = 1$ $i \in \{1, 2, 3\}$ and $S_0 = 0.1$. From the approach as described in this section, one obtains for the effective values: $\mathbb{D}_{eff} = 2.4495 \cdot 10^{-3}$, $c_{eff}^{part} = 33$, $c_{eff}^{sol} = 1$. It can be seen that this yields: $S(t) = S_0 - 0.15 \cdot 10^{-2} \cdot \sqrt{t}$. Using the more general approach from section 4 and equations (4.2) and (4.3), one obtains as a solution: $S(t) = S_0 - 0.16 \cdot 10^{-2} \cdot \sqrt{t}$. The difference between the two solutions is small. The approximate solution gives a good order of magnitude for the dissolution kinetics. Figure 1 displays the dissolution curves for both approaches.

6. The numerical method for vector valued Stefan problems

Various numerical methods are known to solve Stefan problems: front-tracking, front-fixing, and fixed-domain methods [10]. In a front-fixing method a transformation of coordinates is used (a special case is the isotherm migration method (IMM)). Fixed domain methods are the enthalpy method (EM) and the variational inequality method (VI). Various methods are compared in [11]. The latter methods (IMM, EM, VI) are only applicable when the concentration is constant at the interface. Since in our problem the concentration varies at the interface we restrict ourselves to a front-tracking method. Front-tracking methods are described in [22], [3], [17], [41], [4], [42], and [16]. Recently a number of promising methods are proposed for multi-dimensional Stefan problems: phase field methods ([6], [7], [38]) and level set methods ([20], [27], [9]).

Our main interest is to give an accurate discretization of the boundary conditions for a one-dimensional Stefan problem. Therefore we use the classical moving grid method of Murray and Landis [22] to discretize the diffusion equations. First an outline of the numerical method is given. In the present paper we generalise the method from [31] to a method which can be used for vector valued Stefan problems.

The equations are solved with a finite difference method in the r and t-direction. A characteristic feature of a front-tracking method is that the interface positions are nodal points in every time-step. So, the position of the grid-points depends on time. An outline of the algorithm is:

1. Compute the concentration profiles solving the nonlinear problem given by (2.1),...,(2.6),(2.8),
2. Predict the positions of S_L and S_R at the new time-step: $S_L(t+\Delta t)$ and $S_R(t+\Delta t)$,
3. Redistribute the grid such that $S_L(t+\Delta t)$ and $S_R(t+\Delta t)$ are nodal points. Linear interpolation is used to approximate the concentrations at the previous time-step on the new grid-points,
4. Return to step 1.

6.1 Discretization of the interior region

In [31] the method is explained using an equidistant grid. For efficiency reasons we use a non-equidistant grid to solve vector valued Stefan problems. The motivation for this is: from theory and numerical experiments it appears that the absolute values of the concentration gradients of the diffusing alloying elements are maximal at the moving boundaries. As the displacement of a free boundary is proportional to the concentration gradient the space discretization in the neighbourhood of this boundary should be very accurate. Therefore a fine discretization grid is chosen near the free boundaries and a coarse grid farther away. A geometrically distributed grid is chosen. As an example consider one free boundary ($S_R(t) = M_R,\ t \in [0,T]$). The grid is distributed such that $\Delta r_l^{j+1} = \beta \Delta r_{l+1}^{j+1}$, with $\beta \leq 1$ and $\Delta r_l^{j+1} := r_{l+1}^{j+1} - r_l^{j+1}$. The resulting discretized equation for one alloying element is given by (for ease of notation we omit here the index i):

$$\frac{c_l^{j+1}}{\mathbb{D}\Delta t} + \{(r_{l+\frac{1}{2}}^{j+1})^a \frac{c_{l+1}^{j+1} - c_l^{j+1}}{\Delta r_l^{j+1}} - (r_{l-\frac{1}{2}}^{j+1})^a \frac{c_l^{j+1} - c_{l-1}^{j+1}}{\Delta r_{l-1}^{j+1}}\} / \{(r_l^{j+1})^a (\Delta r_l^{j+1}/2 + \Delta r_{l-1}^{j+1}/2)\} =$$

$$\frac{1}{\mathbb{D}\Delta t}\{c_l^j + \frac{c_{l+1}^j - c_{l-1}^j}{\Delta r_l^{j+1} + \Delta r_{l-1}^{j+1}}(r_l^{j+1} - r_l^j)\}, \tag{6.1}$$

where c_l^j approximates the concentration $c(r_l^j, j\Delta t)$. For more details we refer to [29] pp. 255-261.

6.2 Discrete boundary condition at a moving boundary

For the case of two moving boundaries, i.e. $M_L < S_L(t)$ and $S_R(t) < M_R,\ t \in [0,T]$, the solutions of the diffusion equations are formally determined by the concentrations of all alloying elements at the boundaries S_L and S_R. So a change of a concentration at S_L influences the solution of the diffusion equations and hence the gradients of concentration at S_R (and vice versa). However, it has been shown in [31] that for Δt sufficiently small the concentrations at $(j+1)\Delta t$ in the vicinity of S_L are not influenced by the concentrations at $(j+1)\Delta t$ in the vicinity of S_R. An explanation is given using the theory of penetration. In most applications Δt is already chosen less than this bound for accuracy reasons. So in this section we assume that the boundary conditions on both moving boundaries are independent.

The boundary conditions are discretized with virtual grid-points. The virtual concentrations are eliminated by (6.1). For ease of notation we only consider S_L and assume that $\Phi_L = \{1, ..., n\}$ and $S_R(t) = M_R$. All concentrations which satisfy (6.1) and the boundary conditions on M_R are functions of $c_{i,0}^{j+1},\ i \in \{1, ..., n\}$, which is the concentration of alloying element Sp_i at S_L. To determine these remaining unknowns one has to solve the following nonlinear equations:

$$f_i(c_{i,0}^{j+1}, c_{i+1,0}^{j+1}) := \mathbb{D}_i(c_{i+1}^{part} - c_{i+1,0}^{j+1})(c_{i,1}^{j+1} - c_{i,-1}^{j+1}) - \mathbb{D}_{i+1}(c_i^{part} - c_{i,0}^{j+1})(c_{i+1,1}^{j+1} - c_{i+1,-1}^{j+1}) = 0, \tag{6.2}$$

for $i \in \{1, ..., n-1\}$ and

$$f_n(c_{1,0}^{j+1}, ..., c_{n,0}^{j+1}) := \Pi_{i=1}^{n}(c_{i,0}^{j+1})^{m_i} - K_L = 0. \tag{6.3}$$

To approximate a root for the vector function $(f_1, ..., f_n)^T$ we use the Newton-Raphson method:

$$\begin{pmatrix} c_{1,0}^{j+1}(p+1) \\ \vdots \\ c_{n,0}^{j+1}(p+1) \end{pmatrix} = \begin{pmatrix} c_{1,0}^{j+1}(p) \\ \vdots \\ c_{n,0}^{j+1}(p) \end{pmatrix} + (J(p))^{-1} \cdot \begin{pmatrix} -f_1(p) \\ \vdots \\ -f_n(p) \end{pmatrix}, \tag{6.4}$$

where J is the Jacobian and the p-th iterate of the concentration is denoted by $c_{i,0}^{j+1}(p)$. The matrix J is sparse. Only the matrix elements of the last row and the elements $J_{i,i}$ and $J_{i,i+1},\ i \in \{1, ..., n-1\}$ are non-zero. In practice it is impossible to compute the first $n-1$ rows of J. Therefore we use a discrete approximation $\hat{J}$. The elements of $\hat{J}$ are obtained from:

$$\hat{J}_{i,i} = [f_i(c_{i,0}^{j+1} + \varepsilon, c_{i+1,0}^{j+1}) - f_i(c_{i,0}^{j+1} - \varepsilon, c_{i+1,0}^{j+1})]/2\varepsilon,\ i \in \{1, ..., n-1\},$$

$$\hat{J}_{i,i+1} = [f_i(c_{i,0}^{j+1}, c_{i+1,0}^{j+1} + \varepsilon) - f_i(c_{i,0}^{j+1}, c_{i+1,0}^{j+1} - \varepsilon)]/2\varepsilon,\ i \in \{1, ..., n-1\}.$$

Note that ε has to be sufficiently small, but larger than the accuracy of the numerical scheme to evaluate the concentrations. The computation of $\hat{J}$ requires that in every Newton-Raphson iteration the discretized equations have to be solved $2(n-1)$ times (also when $S_R(t) < M_R$).

To start the Newton-Raphson procedure an initial guess has to be found. To prevent convergence to an undesired root, the initial guess is chosen as close as possible to the root. For time-steps $j > 1$, the boundary concentrations from the former time-step are chosen as initial guesses. However, at time-step $j = 1$, the analytical approximations are used. We terminate the iteration when

$$\sum_{i=1}^{n} |c_{i,0}^{j+1}(p+1) - c_{i,0}^{j+1}(p)| < \varepsilon.$$

6.3 Adaptation of the moving boundaries

We have not used all boundary conditions given in (2.7) to determine the concentrations. The remaining conditions are used to adapt the positions of the moving boundaries. In [31] the

Euler Forward and Trapezium time integration methods are described to determine the moving boundary positions. The Trapezium method is preferred because the costs per iteration are the same for both methods, but the results obtained with the Trapezium method are more accurate [31]. For the solution of a vector valued Stefan problem we have implemented the Trapezium integration method iteratively, simultaneously with the Newton-Raphson iteration to obtain $c_{i,0}^{j+1}$. The iteration is terminated when

$$\sum_{i\in\Phi_L} |c_{i,0}^{j+1}(p+1) - c_{i,0}^{j+1}(p)| + \frac{|S_L^{j+1}(p+1) - S_L^{j+1}(p)|}{S_L^j - M_L} < \varepsilon.$$

7. Numerical experiments

This section contains some numerical experiments. We, however, omitted experiments to test the accuracy of the numerical calculations. Here we remark only that the accuracy of the time-integration was order $O(\Delta t)$ and the accuracy of the mesh-size was order $O(\Delta r)^2$. For stability reasons we took $\Delta t < 1000\frac{\Delta r^2}{max(\mathbb{D}_i)}$. We refer to [31] for more details. First we compare the solutions obtained with the numerical method, as described in Section 6 with the solutions from the analytical relations of Sections 4 and 5. We also show the behaviour of the concentration profile of the alloying elements. Finally, we show an example of an application of the model in aluminium industry.

7.1 A comparison between the numerical and analytical approaches

The first example treats a system in which the analytical approaches do not differ very much. We have set: $c_i^{part} = 100, c_i^0 = 0, \mathbb{D}_i = i \cdot 10^{-13}, i \in \{1,2,3\}, K = 1, S_0 = 0.1 \cdot 10^{-6} m$. For the finite difference, we set $M_R = 0.1 \cdot 10^{-4} m$. Where we imposed a homogeneous Neumann condition. The position of the moving boundary, $S(t)$, has been sketched as a function of time in Figure 2.

In Figure 2 we sketched three analytical approaches: the formal analytical approach from equations (4.2,4.3) and both the upper- and lower bounds for the dissolution kinetics as given in equation (4.5). It can be seen that the analytical approaches hardly differ. This is because $c_i^{part} >> c_i^{sol}$. It can also be seen that the results from the numerical approach matches perfectly with the results from the analytical approaches at the early stages. However, at the later stages, from $t > 150$, the approaches start to differ significantly. This is due to the fact that the primary phase, in which we have diffusion, starts to saturate: the concentration profiles start to flatten. To illustrate this behaviour, the concentration profiles of all the alloying elements have been sketched at $t = 50$ and $t = 200$, respectively in Figures 3 and 4.

It is clear that at $t = 50$ the concentration of the chemical elements is hardly influenced yet. Up to then, the numerical- and analytical approaches match perfectly (see Figure 2). It can be seen that at $t = 200$ the concentration of the alloying elements at M_R starts to increase. The profiles flatten and the dissolution kinetics are delayed compared to the analytical approaches for the unbounded domain. This agrees well with Proposition 4.1. in section 4.

In the second example we maintained the settings of the first example except for the particle concentrations: $c_i^{part} = 20, i \in \{1,2,3\}$ and $M_R = 0.2 \cdot 10^{-5}$. The results have been sketched in Figure 5.

It can be seen in Figure 5 that the analytical approaches differ more than in the preceeding example. The lower and upper limit correspond to respectively curves 1 and 3. These represent the limits given in equation (4.5). The exact analytical approach, represented by curve

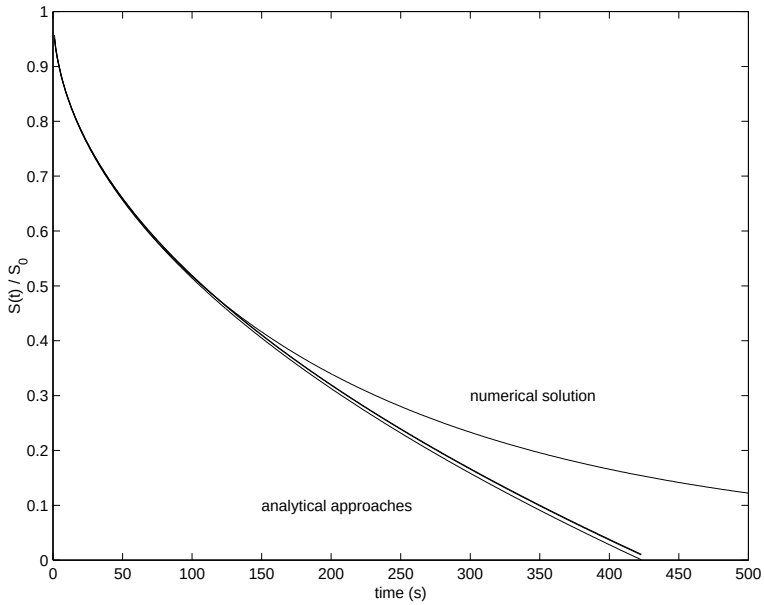

Figure 2: A comparison between a numerical- and analytical approach.

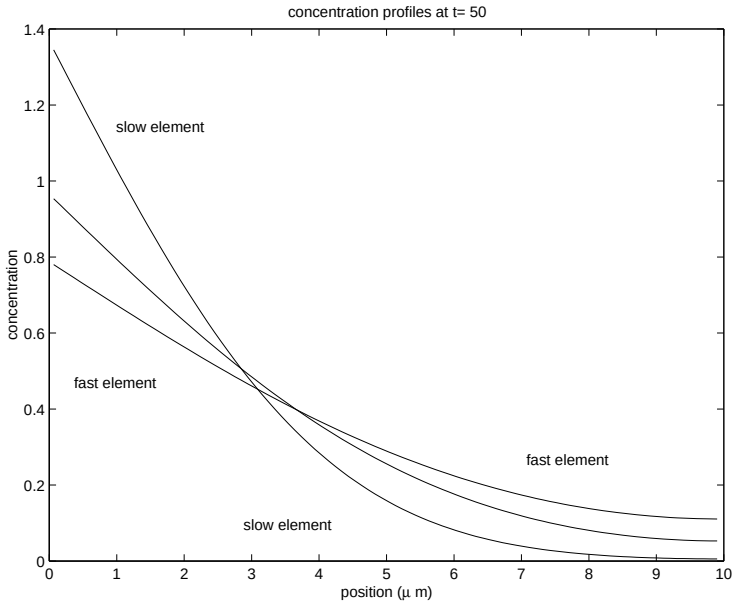

Figure 3: Concentration profiles of the chemical elements at $t = 50$.

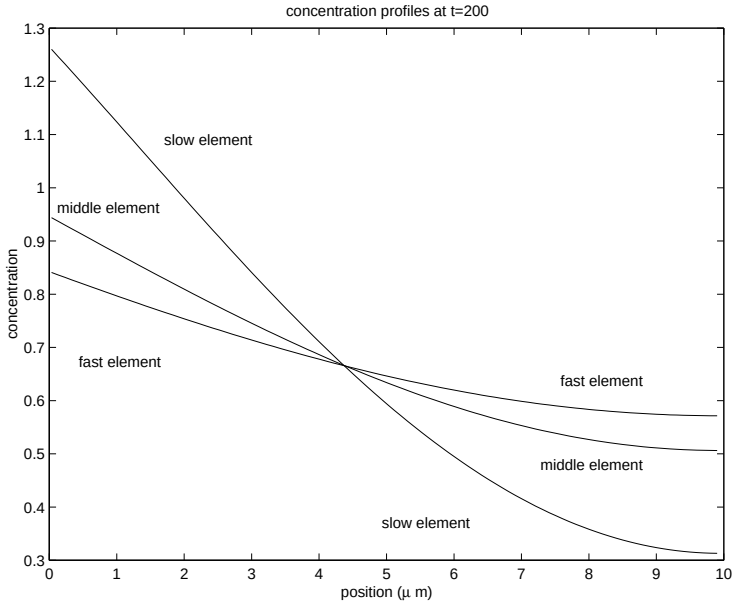

Figure 4: Concentration profiles of the chemical elements at $t = 200$.

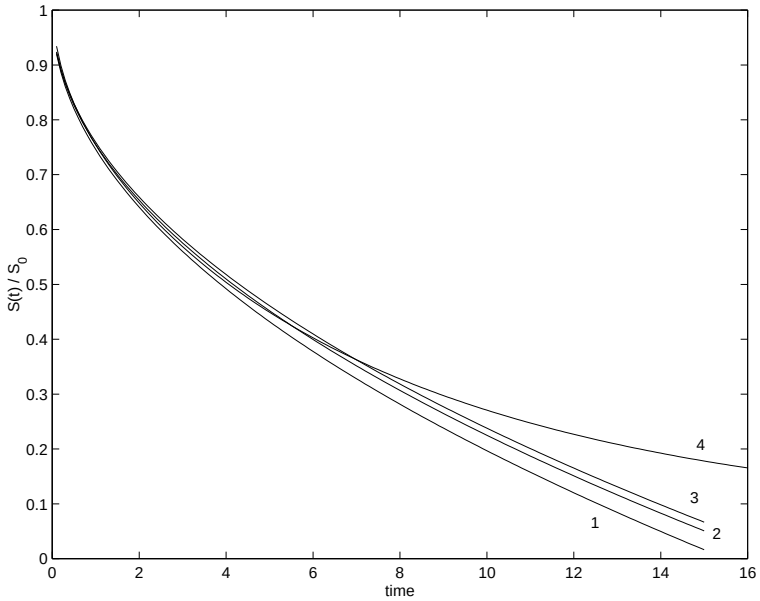

Figure 5: A comparison between a numerical- and analytical approach. Curve 1: Lower bound, Curve 2: Analytical solution, Curve 3: Upper bound, Curve 4: Numerical solution

2, falls just within the limits and so does the numerical approach. The numerical approach is given by curve 4. It can however, be seen that the numerical approach and exact analytical approach for the unbounded domain differ a little. This is attributed to the numerical inaccuracy. The numerical solution is between the limits. At the later stages it can be seen that the numerical and analytical approach start to deviate significantly. This is again attributed to the saturation of the primary phase. From the experiments it may be seen that the analytical approaches provide a good order of magnitude for the dissolution kinetics as long as the concentration at the fixed boundary does not change significantly. In other words, if the overall concentration is low enough, then the overall dissolution times as predicted from the analytical approaches give a good order of magnitude for the dissolution rate and time. These limits may then be well used for engineering purposes.

7.2 The quasi-binary and multicomponent approach compared

For the same two configurations as in the preceeding subsection, we look at the quasi-binary and multicomponent approach. With the quasi-binary approach, we mean the Finite Difference calculations, in which we incorporate the effects of the finite cell dimensions, done with the so-called effective diffusion coefficient, effective interface and particle concentration.

Figure 6 presents the calculations done for the first case of the preceeding subsection, i.e. the particle concentration is 100 for all chemical elements. It can be seen that the difference between the quasi-binary and multi-component approach is negligible. The same calculations have been done for the case that the particle concentration is 20 for all chemical elements. The results are shown in Figure 7. As can be expected from the theory, the difference between the calculations is larger now. Nevertheless, the calculations, still do provide a good order of magnitude. This quasi-binary approach may be used to test the numerical calculations for the multi-component algorithm for cases in which the cell radius is not large. Moreover, the quasi-binary approach can be used well as an engineering solution for the case that no multi-component algorithm is available.

For completeness it is noted that all the theory about the quasi-binary approach is only valid for the case that the geometry is planar, although we expect that it is also a suitable approach for other geometries.

7.3 A spherical example with 5 alloying elements

An example of an application of the model to 5 alloying elements is given in Figure 8. Figure 8 displays the interface position as a function of time for a spherical geometry. We chose $c_i^{part} = 20, S_0 = 1 \cdot 10^{-6}, M_R = 5 \cdot 10^{-6}$ and $\mathbb{D}_i = i \cdot 10^{-13}, i \in \{1, ..., 5\}$. It can be seen that the shape of the curve differs from the planar geometry. This difference is due to the curvature of the moving boundary: during dissolution the moving boundary area decreases, whereas this area remains constant for the planar case. It may also be noted that the interface position does not assume a square-root like behaviour as in the case of a planar particle. This characteristic can be observed for cylindrical and spherical geometries.

Another characteristic that can be observed for curvilinear geometries is the dependency of the interface concentrations on time (see Figure 9). The increase of the interface concentrations is physically interpreted as an accumulation of the slower alloying elements on the interface. These slower alloying elements diffuse at a slower rate from the interface deeper into the primary phase.

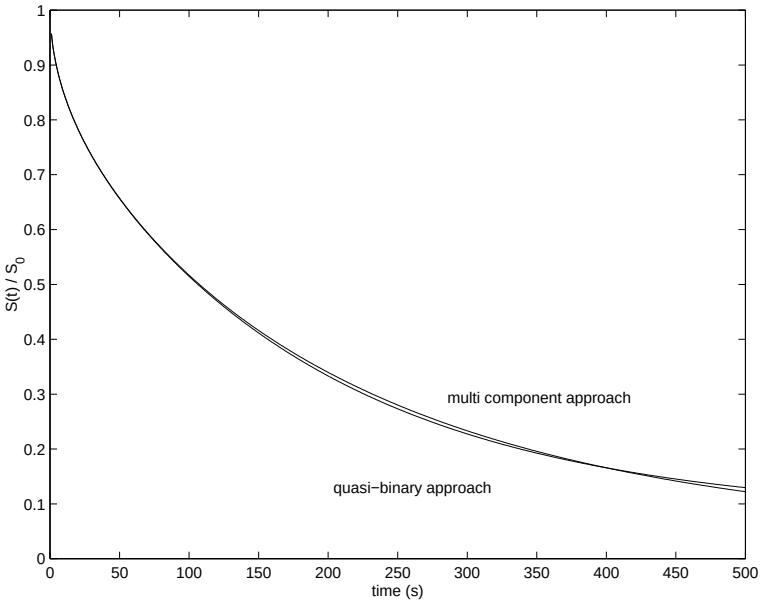

Figure 6: The interface position as a function of time for the quasi-binary and multi-component approach for a dissolving plane with three chemical elements. The particle concentration, $c^{part} = 100$.

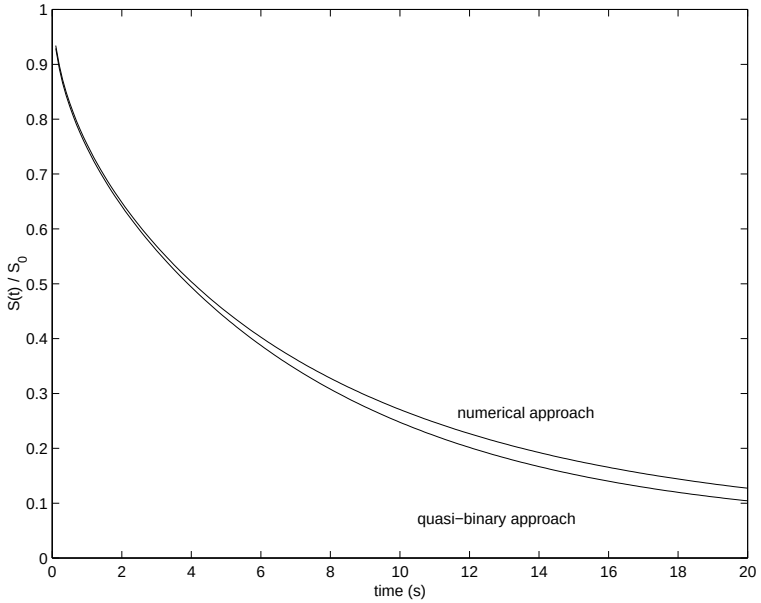

Figure 7: The interface position as a function of time for the quasi-binary and multi-component approach for a dissolving plane with three chemical elements. The particle concentration, $c^{part} = 20$.

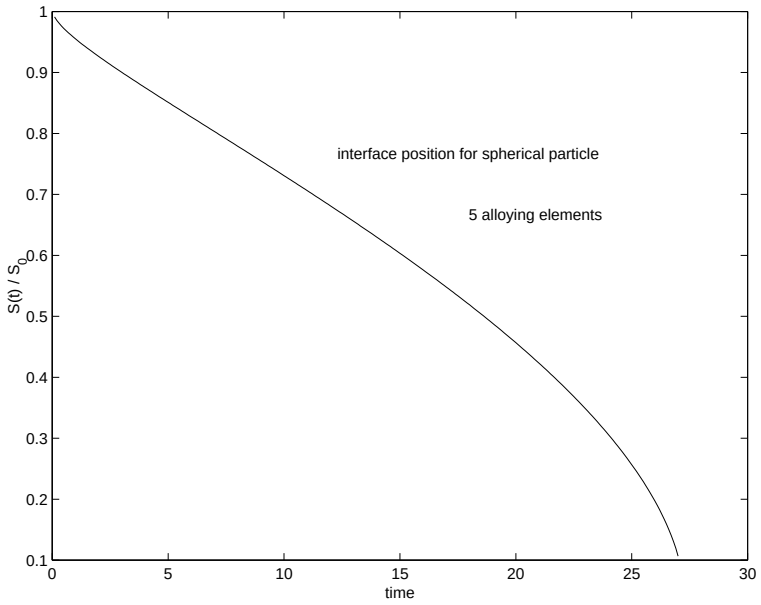

Figure 8: The interface position as a function of time for a dissolving sphere with 5 alloying elements.

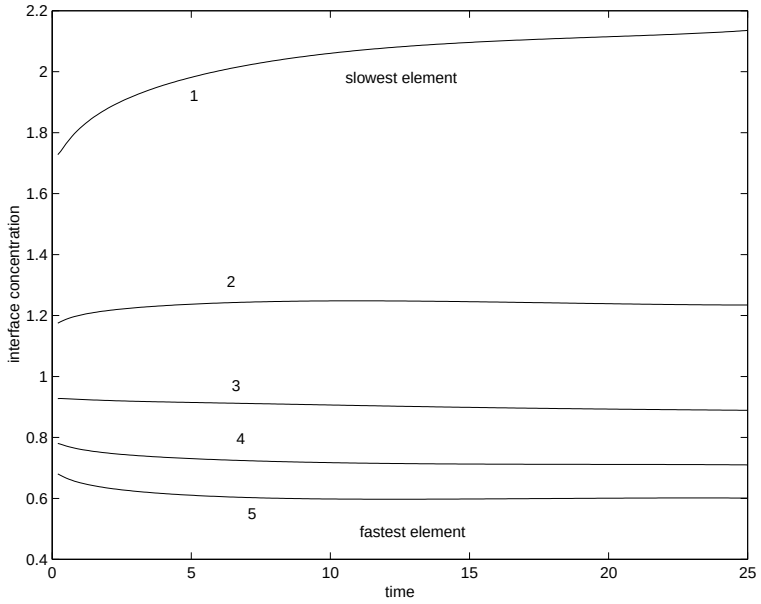

Figure 9: The interface concentrations as a function of time.

7.4 An industrial example with a three-component system

As an industrial example of the mathematical model, we look at a three phase system. We consider the simultaneous dissolution of a Si-particle and a Mg_2Si-particle in an Al-alloy. The silicon-particle is in the center of the spherical cell in which we consider the dissolution. The Si-particle is enclosed by the aluminium-rich phase (primary phase), which is enclosed by a Mg_2Si-phase. We also have incorporated a temperature-time profile, which is common in aluminium industry. The alloy is heated from 300 K up to 823 K with a heat-up rate of 0.05 K/s. The initial concentration in the primary phase is: $c^0_{Si} = 0, c^0_{Mg} = 0.04$, whereas the particle concentrations are given by:$c^{part}_{Si,L} = 100, c^{part}_{Si,R} = 35$ and $c^{part}_{Mg,R} = 65$. For the diffusion coefficients of silicon and magnesium, we respectively have: $\mathbb{D}_{Si} = 2.02 \cdot 10^{-4}$ and $\mathbb{D}_{Mg} = 0.49 \cdot 10^{-4}$. Then for the solubility product of silicon and magnesium in aluminium, we have $K = 4.03 \cdot 10^{-5} \cdot exp(\frac{74488}{8.3 \cdot \tau})$, in which τ is the temperature. For the solubility of silicon in aluminium, we have used the discrete data from [21].

We here are dealing with three components. We assume that no magnesium diffuses into the silicon-particle, i.e. we impose a homogeneous Neumann-condition for magnesium at boundary S_L. Due to the homogeneous Neumann condition at S_L, magnesium accumulates at this boundary. For the case that the concentration of magnesium at the boundary of the silicon particle (S_L) is low enough, one can use the solubility of silicon in pure aluminium, given by binary phase diagrams. If, however, magnesium accumulates up to a certain threshold value, the concentration of silicon at the boundary S_L has to satisfy the hyperbolic relationship of the solubility of silicon and magnesium in aluminium. In a more mathematical notation, we thus write for the silicon concentration at the boundary S_L:

$$c^{sol}_{Si} = \frac{K_{Mg_2Si}}{c_{Mg}(S_L(t),t)^2} \cdot H(c_{Mg}(S_L(t),t) - \tilde{C}) + K_{Si} \cdot H(\tilde{C} - c_{Mg}(S_L(t),t)). \tag{7.1}$$

In which H represents the heavy-side function and the threshold concentration $\tilde{C}$ follows from the continuity of the above relation (7.1), i.e.:

$$\tilde{C} = \sqrt{\frac{K_{Mg_2Si}}{K_{Si}}}.$$

Note that K_{Mg_2Si} and K_{Si} are functions of temperature and hence so is $\tilde{C}$. The results of the experiments with the simultaneous dissolution of a Si- and Mg_2Si-particle are shown in Figure 7.4 and 7.4.

It can be seen from Figure 7.4 that both the silicon and magnesium concentration at the boundary S_R increase with time. This is due to the temperature increase. When the temperature is constant (833 K, $t = 2.05 \cdot 10^4$), the concentrations at the boundary S_R stay approximately constant. It can also be seen that the silicon concentration at S_L starts to increase very rapidly after approximately $1.6 \cdot 10^4$ seconds. Once the temperature is fixed, the Si-concentration at S_L is fixed as well, until the magnesium concentration has passed the so-called threshold concentration $\tilde{C}$ (at $t = 2.7 \cdot 10^4$). The Si-concentration then starts to decrease according to equation (7.1). We only have shown the most interesting part of the calculation ($t \in (0, 3.1 \cdot 10^4]$). The evolution of the moving boundary positions is shown in Figure 7.4. Note that due to the jump in the functional dependency in equation (7.1), the $S_L(t)$ may have a discontinuous time derivative.

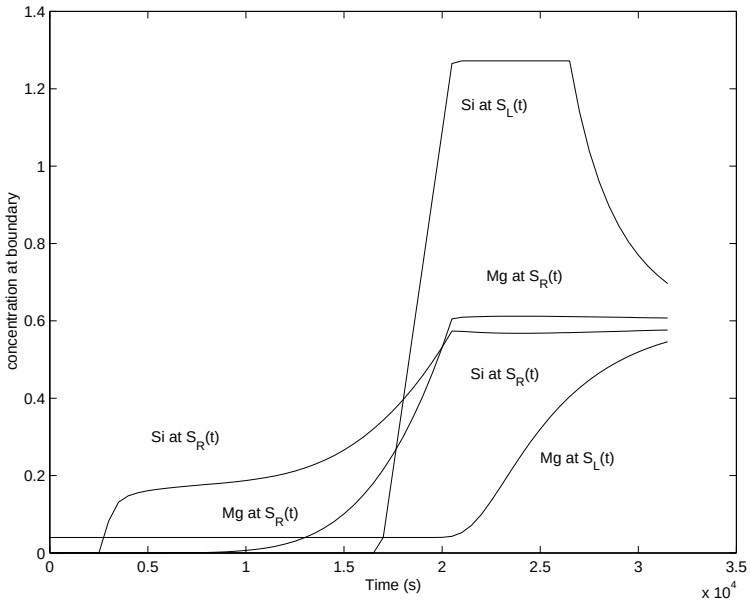

Figure 10: The concentrations at the moving boundary as a function of time.

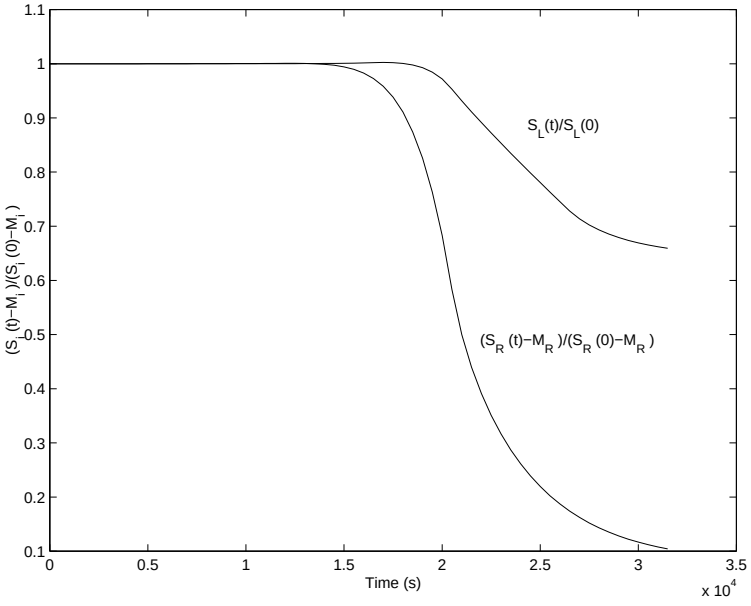

Figure 11: The moving boundary positions as a function of time.

8. Conclusions

A mathematical model is presented to describe the dissolution of stoichiometric multi-component particles in multi-component alloys. Some results concerning existence and uniqueness are given.

A definition is introduced about mass-conserving solutions to Stefan problems. It is proven in $\mathbb{R}^d$ for the scalar Stefan problem that no solution exists if:

$$(c^{part} - c^0)(c^{part} - c^{sol}) \leq 0, \;\; c^{sol} \neq c^0 \;\; and \;\; c^0, c^{sol}, c^{part} \in \mathbb{R}^+ \cup \{0\}.$$

For a planar particle dissolving in an unbounded domain, a self-similar solution is used for the scalar Stefan problem. This exact self-similar solution is extended to the dissolution of a multi-component particle. From the exact similarity solution two limits have been derived for the dissolution of a planar particle in an unbounded domain. The limits are easy to calculate and provide good insight into the dissolution kinetics and can therefore be used for engineering purposes as well.

For the case of initial concentrations equal to zero, a simple expression is derived for the dissolution in terms of an effective diffusion coefficient. It turns out that the effective diffusion coefficient is equal to a geometric mean of all diffusion coefficients involved. The weight-factors come from the particle concentrations.
Furthermore, a numerical method is presented to deal with more general cases: curvilinear co-ordinates and two boundaries. It has been shown that the results of the numerical method agree well with the results obtained from the analytical approaches for the planar case as long as the solution at the fixed boundary did not change significantly from the initial condition.

Still, a number of open questions remain:

- For the vector valued Stefan problem, multiple solutions may exist [32], further research is needed at this point,
- Is the model valid when blow up occurs?

9. Appendix 1: The maximum principle for a discontinuity at the boundary

Below we give a generalisation of the maximum principle given in [25]. This generalisation is done for the case that we have $S(t)$ and M respectively as the left and right boundaries. Moreover, we only consider the one-dimensional case because this reasoning can be extended easily to the d-dimensional case.

Theorem (maximum principle)

Suppose $S \in C[0,T]$ and $\Omega(t) = \{r \in \mathbb{R} | S(t) < r < M\}$. Consider the bounded function $c \in C^{2,1}(Q) \cap C(\bar{Q})$, where expression (2) holds in points where the boundary functions are discontinuous. Note that $\Omega(t)$ may be an unbounded domain ($M = \infty$). When c satisfies:

$$\frac{\partial c}{\partial t} - \frac{\partial^2 c}{\partial r^2} = 0, \;\; r \in (S(t), M), \;\; t \in (0, T]$$

then

$$min\{inf_{r \in \Omega(0)} \; c(r,0), inf_{t \in [0,T]} \; c(S(t),t)\} \leq c(r,t) \leq$$

$max\{sup_{r\in\Omega(0)}\ c(r,0), sup_{t\in[0,T]}\ c(S(t),t)\}$ for $(r,t)\in(\bar{Q})$.

Proof

The maximum principle is first proved for a discontinuous function c and thereafter generalised to unbounded domains.

We first consider the second inequality for a bounded domain ($M<\infty$). Define $\mu = max\{sup_{r\in\Omega(0)}\ c(r,0), sup_{t\in[0,T]}\ c(S(t),t)\}$. Suppose there is a point $(\xi,\tau)\in Q$ such that $\mu_1 := c(\xi,\tau) > \mu$. Take a neighbourhood B of $(S(0),0)$ such that $c(r,t)\leq\mu+\frac{1}{2}(\mu_1-\mu)$ for $(r,t)\in B$, which is always possible because expression (2) is valid in $(S(0),0)$. Furthermore B is such that $(\xi,\tau)\in Q\backslash B$. Since c is a continuous function in $Q\backslash B$ the maximum principle given by [25] can be applied. From this it follows that $c(r,t)\leq\mu+\frac{1}{2}(\mu_1-\mu)$, for $(r,t)\in Q\backslash B$ which leads to a contradiction. The first inequality can be proved in a similar way. This proves the theorem for a discontinuous function c. □

It is easy to generalise the maximum principle on a bounded domain to an unbounded domain when the function c is bounded (compare the proof of Lemma 2.4, p. 18 in [37]).

References

1. H.B. Aaron and G.R. Kotler. Second phase dissolution. *Metallurgical Transactions*, 2:393–407, 1971.
2. U.L. Baty, R.A. Tanzilli, and R.W. Heckel. Dissolution kinetics of CuAl2 in an Al-4Cu alloy. *Metallurgical Transactions*, 1:1651–1656, 1970.
3. R. Bonnerot and P. Jamet. A second order finite element method for the one-dimensional Stefan problem. *Int. J. Num. Meth. Engng*, 8:811–820, 1974.
4. K. Brattkus and D.I. Meiron. Numerical simulations of unsteady crystal growth. *SIAM J. Appl. Math.*, 52:1303–1320, 1992.
5. M. Brokate, N. Kenmochi, I. Müller, J.F. Rodriguez, and C. Verdi. *Phase transitions and hysteresis; lectures given at the 3rd session of the Centro Internazionale Matematico Estivo (CIME) held in Montecatini Terme, Italy, July 13-21, 1993.* Lecture notes in mathematics 1584. Springer, Berlin, 1994.
6. G. Caginalp. An analysis of a phase field model of a free boundary. *Arch. Rat. Mech. Anal.*, 92:205–245, 1986.
7. G. Caginalp and J.T. Lin. A numerical analysis of an anisotropic phase field model. *IMA J. Appl. Math.*, 39:51–66, 1987.
8. J. Chadam and H. Rasmussen. *Free boundary problems involving solids.* Longman Scientific & Technical, Harlow, 1993.
9. S. Chen, B. Merriman, S. Osher, and P. Smereka. A simple level set method for solving Stefan problems. *J. Comp. Phys.*, 135:8–29, 1997.
10. J. Crank. *Free and Moving Boundary Problems.* Clarendon Press, Oxford, 1984.
11. A.J. Dalhuijsen and A. Segal. Comparison of finite element techniques for solidification problems. *Int. J. Num. Meth. Engng.*, 23:1807–1829, 1986.
12. A. Friedman. *Partial differential equations of parabolic type.* Prentice-Hall, INC, Englewood Cliffs, N.J., 1964.
13. J. Ågren. Diffusion in phases with several components and sublattices. *J. Phys. Chem.*

Solids, 43:421–430, 1981.

14. J.M. Hill. *One-dimensional Stefan Problems: an Introduction*. Pitman Monographs and Surveys in Pure and Applied Mathematics 31. Longman Scientific & Technical, New York, 1987.
15. Roger Hubert. Modelisation numerique de la croissance et de la dissolution des precipites dans l'acier. *ATB Metallurgie*, 34-35:5–14, 1995.
16. D. Juric and G. Tryggvason. A front-tracking method for dendritic solidification. *J. Comput. Phys.*, 123:127–148, 1996.
17. P. Lesaint and R. Touzani. Approximation of the heat equation in a variable domain with application to the Stefan problem. *Siam J. Num. Anal.*, 26:366–379, 1989.
18. E. Magenes, C. Verdi, and A. Visintin. Theoretical and numerical results on the two-phase Stefan problem. *SIAM J. Num. Anal.*, 26:1425–1438, 1989.
19. A.M. Meirmanov. *The Stefan problem*. De Gruyter Expositions in Mathematics, Vol 3. Walter de Gruyter, Berlin, 1992.
20. B. Merriman, J.K. Bence, and S.J. Osher. Motion of multiple functions: a level set approach. *J. Comput. Phys.*, 112:334–363, 1994.
21. L.F. Mondolfo. *Aluminium Alloys, structure and properties*. Butterworth, London, 1976.
22. W.D. Murray and F. Landis. Numerical and machine solutions of transient heat-conduction problems involving melting or freezing. *Trans. ASME (C) J. Heat Transfer*, 81:106–112, 1959.
23. F.V. Nolfi Jr., P.G. Shewmon, and J.S. Foster. The dissolution and growth kinetics of spherical precipitates. *Transactions of the Metallurgical Society of AIME*, 245:1427–1433, 1969.
24. R.L. Parker. Crystal growth mechanisms: energetics, kinetics and transport. *Solid State Physics*, 25:152–298, 1970.
25. M.H. Protter and H.F. Weinberger. *Maximum Principles in Differential Equations*. Prentice-Hall, Englewood Cliffs, 1967.
26. O. Reiso, N. Ryum, and J. Strid. Melting and dissolution of secondary phase particles in AlMgSi-alloys. *Met. Trans. A*, 24A:2629–2641, 1993.
27. J.A. Sethian. *Level set methods; evolving interfaces in geometry, fluid mechanics, computer vision, and materials science*. Cambridge monographs on applied and computational mathematics 3. Cambridge University Press, Cambridge, 1996.
28. U.H. Tundal and N. Ryum. Dissolution of particles in binary alloys: Part I. computer simulations. *Metallurgical Transactions*, 23A:433–449, 1992.
29. F. Vermolen. *Mathematical Models for Particle Dissolution in Extrudable Aluminium Alloys*. PhD thesis, Delft University of Technology, The Netherlands, 1998.
30. F.J. Vermolen and S. Van der Zwaag. A numerical model for the dissolution of spherical particles in binary alloys under mixed mode control. *Materials Science and Engineering A*, 220:140–146, 1996.
31. Fred Vermolen and Kees Vuik. A numerical method to compute the dissolution of second phases in ternary alloys. *Journal of computational and applied mathematics*, 93:123–143,

1998.

32. Fred Vermolen and Kees Vuik. *A vector valued Stefan problem from aluminium industry.* MAS-R9814. Centrum voor Wiskunde en Informatica, Amsterdam, July 1998. CWI-report.
33. Fred Vermolen, Kees Vuik, and Sybrand van der Zwaag. The dissolution of a stoichiometric second phase in ternary alloys: a numerical analysis. *Materials Science and Engineering A*, A246:93–103, 1998.
34. Fred Vermolen, Kees Vuik, and Sybrand van der Zwaag. A mathematical model for the dissolution kinetics of Mg_2Si-phases in $Al-Mg-Si$ alloys during homogenisation under industrial conditions. *Materials science and engineering*, A254:13–32, 1998.
35. A. Visintin. *Models of Phase Transitions.* Progress in Nonlinear Differential Equations and Their Application: 28. Birkhäuser, Boston, 1996.
36. J.M. Vitek, S.A. Vitek, and S.A. David. Modelling of diffusion controlled phase transformation in ternary systems and application to the Ferrite/Austenite transformation in the Fe-Cr-Ni-system. *Met. Trans. A*, 26A:2007–2025, 1995.
37. C. Vuik. *The solution of a one-dimensional Stefan problem.* 90. CWI-tract, CWI-Amsterdam, 1993.
38. S-L. Wang and R.F. Sekerka. Algorithms for phase field computation of the dentritic operating state at large supercoolings. *J. Comput. Phys.*, 127:110–117, 1996.
39. H. Weber. *Die partiellen Differential-Gleichungen der mathematischen Physik II.* Vieweg, Braunschweig, 1901.
40. M.J. Whelan. On the kinetics of particle dissolution. *Metal Science Journal*, 3:95–97, 1969.
41. D.E. Womble. A front-tracking method for multiphase free boundary problems. *SIAM J. Numer. Anal.*, 26:380–396, 1989.
42. M. Zerroukat and C.R. Chatwin. *Computational moving boundary problems.* Applied and engineering mathematics series 8. John Wiley, New York, 1994.